

# Effect of Molecular Dissociation and Sorbent Carbonization on Bisolute Sorption of Pharmaceuticals by Biochars

Lin Wu · Binghua Li · Erping Bi

Received: 12 February 2017 / Accepted: 31 May 2017 / Published online: 10 June 2017  
© Springer International Publishing AG Switzerland 2017

**Abstract** Understanding the sorption behavior of mixtures of pharmaceuticals is critical for predicting their environmental behavior and for risk assessment. Experiments on ketoprofen (KTP) and triclosan (TCS) sorption by wheat straw-derived biochars at 300 °C (WS300) and 700 °C (WS700) in single solute and bisolute systems were conducted to probe the sorption mechanisms. The results of the single solute sorption indicated that WS700 with higher degree of carboniza-

tion had higher sorption coefficient ( $K_d$ ) and nonlinearity than WS300. In a bisolute system, no competitive effect was observed for partition of neutral KTP and TCS in the noncarbonized phase of WS300, but they competed for the adsorptive sites on the carbonized phase of WS300 and WS700 for sorption, in which  $\pi$ - $\pi$  interaction is proposed as the main mechanism. The competition in the bisolute system varied with degree of dissociation of KTP and TCS, and led to a lower and less nonlinear sorption compared with that in the single solute system. TCS was more competitive than KTP due to its higher hydrophobicity, and sorption inhibition of KTP was enhanced with increasing TCS concentration. Degree of both molecular dissociation and sorbent carbonization should be considered in bisolute sorption of organic pollutants by biochars.

**Highlights** • Noncompetitive partition can occur in the noncarbonized phase of WS300.

- KTP and TCS competed for sorption sites on the carbonized phase of biochars.
- Competitive sorption varied with degree of dissociation of KTP and TCS.
- TCS was more competitive than KTP due to its higher hydrophobicity.

**Electronic supplementary material** The online version of this article (doi:10.1007/s11270-017-3424-3) contains supplementary material, which is available to authorized users.

L. Wu · E. Bi (✉)

School of Water Resources and Environment, and Beijing Key Laboratory of Water Resources and Environment Engineering, China University of Geosciences (Beijing), Beijing 100083, China  
e-mail: bi@cugb.edu.cn

L. Wu

e-mail: wulin@cugb.edu.cn

B. Li

Beijing Water Science and Technology Institute, Beijing 100048, China  
e-mail: libinghua75@163.com

**Keywords** Pharmaceuticals · Dissociation · Biochar · Carbonization · Bisolute sorption

## Abbreviations

KTP	Ketoprofen
TCS	Triclosan
WS	Wheat straw
PPCPs	Pharmaceuticals and personal care products
HPLC	High performance liquid chromatograph
SSA	Specific surface area
FTIR	Fourier transform infrared
SEM	Scanning electron microscope
pH <sub>PZC</sub>	Point of zero charge

## 1 Introduction

The increasing public and scientific concern over pharmaceuticals and personal care products (PPCPs) can be attributed to alarming evidence from scientific literature indicating their potential risk to the ecological system and human health (Daughton and Ternes 1999; Tijani et al. 2013; Dodgen et al. 2016). Knowledge on the sorption of PPCPs in the environment is critical for their transport and risk assessment. As the presence of various PPCPs in an area is very common in the real environment and the interactions between them may alter their environmental behavior and health risks greatly, research on the sorption of mixtures of PPCPs needs to be strengthened in order to establish a more accurate modeling scheme for environmental risk assessment of PPCPs (Jung et al. 2015; Kočárek et al. 2016).

Several mechanisms for bisolute sorption of organic compounds including PPCPs have been reported, including strong competitive sorption on the same sorption sites (Yu and Huang 2005), noncompetitive sorption onto partition-dominated sorbents (Xing et al. 1996), and noncompetitive sorption due to complementary adsorption on different sorption sites (Pan and Xing 2010). Furthermore, enhanced sorption in the presence of cosolute has also been reported (Chen et al. 2012b). To summarize, bisolute sorption characteristics of organic compounds are related to the physicochemical properties of sorbates and sorbents and are diverse.

Biochar is a carbonaceous product obtained by pyrolyzing biomass under oxygen-limited conditions. It is intended to be applied to soils for both agricultural gains and carbon sequestration (Tan et al. 2015). Research has shown that biochar can be an effective sorbent for sorption of different types of organic pollutants including PPCPs in the environment, and pyrolysis temperature is considered to be a key factor that controls the nature of biochar and its sorption properties (Chen and Chen 2009; Xiao et al. 2014; Kumari et al. 2014; Cederlund et al. 2016). To sum up, biochar produced at low pyrolysis temperatures is not fully carbonized and sorption of neutral organic pollutants to them is controlled by partition (Chen et al. 2008; Chen et al. 2012a). Biochar produced at relative high temperatures is well carbonized and adsorption is the main sorption mechanism (Keiluweit and Kleber 2009; Chen et al. 2012a). In general, biochar consists of both carbonized and noncarbonized phases in a wide range of pyrolysis temperature; therefore, sorption mechanisms include

both partition and adsorption and the overall sorption can be described by a dual-mode model (Chen et al. 2008). It should be noted that partition and adsorption characteristics of biochar in the single solute system was widely reported, but sorption mechanisms of biochar in the bisolute system is not well understood since diverse mechanisms for bisolute sorption by biochars produced at different pyrolysis temperatures were observed (Chen et al. 2012b; Jung et al. 2015; Wang et al. 2016), and more research is needed to draw definitive conclusions. Furthermore, the research will help implement biochars for environmental applications more effectively.

In this study, ketoprofen (KTP), a nonsteroidal anti-inflammatory and analgesic drug, and triclosan (TCS), a widely used disinfectant, were chosen as model sorbates. They were chosen because these two pharmaceuticals have very different properties such as hydrophobicity and dissociation constants ( $pK_a$ ), and both of them were frequently detected in the environment and have raised serious concern in recent years (Kolpin et al. 2002; Tixier et al. 2003). Previous studies have shown that dissociation greatly affects the sorption of KTP and TCS, and that the sorption is positively related to the organic carbon content and specific surface area of the sorbent (Xu et al. 2009; József et al. 2012; Sigmund et al. 2016). In addition, aqueous solution chemistry (ionic strength and dissolved organic matter) plays an important role in their sorption (Behera et al. 2010; Cho et al. 2011). However, sorption of KTP and TCS in bisolute systems has been little studied. Investigating the bisolute sorption characteristics of KTP and TCS can better understand the environmental behaviors of organic pollutants. Two biochars, produced by pyrolyzing wheat straw (WS) at both a low temperature of 300 °C (WS300) and a high temperature of 700 °C (WS700), were chosen as sorbents representing different degrees of carbonization.

The objective of this study was to investigate the bisolute sorption mechanisms of KTP and TCS by biochars under different degrees of dissociation. The hypothesis was that significant competition between KTP and TCS may occur on WS700 with higher degree of carbonization. However, both noncompetitive partition and competitive sorption would occur on WS300 with lower degree of carbonization due to the existence of both noncarbonized and carbonized phases. Moreover, dissociation of KTP and TCS may reduce their hydrophobicity as well as sorption affinity, thus influence the competitive sorption between them. To this end,

physicochemical properties of biochars were determined, and batch sorption experiments in both single solute and bisolute systems were conducted. Sorption data was fitted by suitable models and analyzed.

## 2 Materials and Methods

### 2.1 Chemicals

Ketoprofen (KTP, >98.0%) and triclosan (TCS, >98.0%) were purchased from Tokyo Chemical Industry (Japan). Solubility ( $S_w$ ) of KTP and TCS is 51 and 10 mg L<sup>-1</sup>, respectively. The molecular sizes (length × width × depth) of KTP and TCS are 9.6 Å × 7.0 Å × 5.0 Å and 9.5 Å × 7.3 Å × 5.0 Å, respectively, calculated by HyperChem 8.0. KTP and TCS can dissociate through the -COOH or -OH groups with p*K*<sub>a</sub> of 4.45 (SRC Physprop Database) and 8.14 (Reiss et al. 2002), respectively. Thus, both KTP and TCS exist in neutral (KTP<sup>0</sup> or TCS<sup>0</sup>) and anionic (KTP<sup>-</sup> or TCS<sup>-</sup>) species (Fig. 1a, b). For a given pH, the fraction ( $\alpha^-$ ) of KTP<sup>-</sup> or TCS<sup>-</sup> can be calculated by (Kah and Brown 2008):

$$\alpha^- = 1 / (1 + 10^{(pK_a - pH)}) \quad (1)$$

The fraction ( $\alpha^0$ ) of KTP<sup>0</sup> or TCS<sup>0</sup> is calculated by:

$$\alpha^0 = 1 - \alpha^- \quad (2)$$

The pH-dependent distribution ratio ( $D_{OW}$ ) representing the change in hydrophobicity upon dissociation (Fig. 1c) is calculated by (Kah and Brown 2008):

$$D_{OW} = K_{OW}^- \cdot \alpha^- + K_{OW}^0 \cdot \alpha^0 \quad (3)$$

where  $K_{OW}^-$  is the octanol-water partition coefficient for KTP<sup>-</sup> or TCS<sup>-</sup>;  $K_{OW}^0$  is the octanol-water partition coefficient for KTP<sup>0</sup> or TCS<sup>0</sup>. log  $K_{OW}^-$  (-1.42 for KTP<sup>-</sup> and -0.57 for TCS<sup>-</sup>) and log  $K_{OW}^0$  (3.17 for KTP<sup>0</sup> and 5.42 for TCS<sup>0</sup>) were calculated by SPARC online calculator (ARChem, USA).

Stock solutions of KTP and TCS were dissolved in methanol from Fisher Chemical Company (Fair Lawn, N.J.) and acetonitrile was obtained from Dikma Technologies Inc. (Lake Forest, CA, USA). Acetic acid and NaCl were bought from Beijing Chemical Works (Beijing, China). Ultrapure water was used in the experiments.

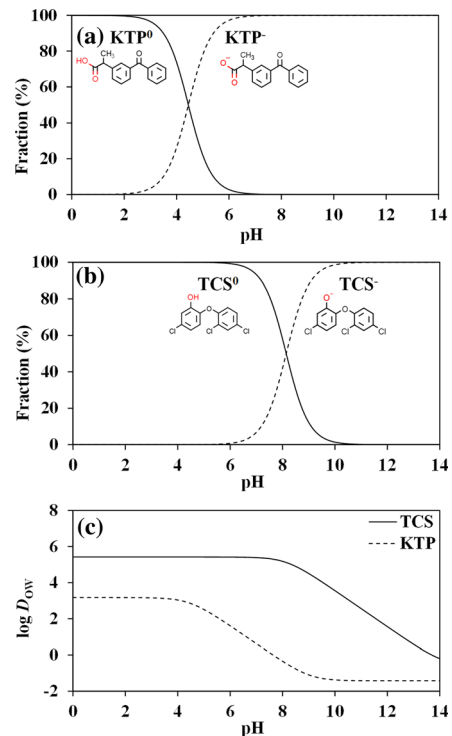


**Fig. 1** Speciation and hydrophobicity of KTP and TCS under different pH conditions

### 2.2 Biochar Preparation and Characterization

Wheat straw (WS) was selected as biomass feedstock. The feedstock was air-dried and smashed into small pieces (0.5–1.5 cm). WS300 and WS700 were produced by pyrolyzing feedstock under oxygen-limited conditions at 300 and 700 °C, respectively (Chen et al. 2008; Xiao et al. 2014). In brief, the feedstock was tightly placed in a ceramic pot, covered with a fitting lid, and then pyrolyzed at a given temperature in a muffle furnace under oxygen-limited atmosphere for 6 h to prevent calcination of the biomass in the presence of oxygen. For demineralization, the resulting charred residues were treated with 1.0 mol L<sup>-1</sup> HCl solution for 24 h. The residues were then washed with deionized distilled water until the pH of the aqueous phase approached neutral. After that, the biochars were oven-dried overnight at 80 °C and passed through a 0.38-mm mesh, and then stored in foil-covered bottle at room temperature (25 ± 1 °C) for subsequent experiments.

The specific surface area (SSA), micropore volume, and average pore width of biochars were measured by N<sub>2</sub> gas adsorption-desorption at the liquid N<sub>2</sub> temperature using a Micromeritics ASAP 2020 M + C (USA).

An Elementar vario EL (Germany) was used to conduct elemental (C, H, N) analyses. Fourier transform infrared (FTIR) spectroscopy to identify the functional groups of biochars was recorded in the 4000–500  $\text{cm}^{-1}$  region (Nicolet iS50, Thermo Scientific, USA). The inner structure and morphology of biochars were determined by a scanning electron microscope (SEM, S-4800, Hitachi, Japan). The surface charge properties of biochars were evaluated by zeta potential measurements, which were conducted at a different equilibrium pH using a Nano-Z Zetasizer (Malvern Instruments Ltd.). Samples were pre-equilibrated in different pH solutions with a solid-to-water ratio the same as sorption experiments.

### 2.3 Batch Sorption Experiments

Single solute and bisolute sorptions were conducted by a batch equilibrium method. Twenty milliliters of sorbate solution (0.01 mol  $\text{L}^{-1}$  NaCl as background electrolyte) was added in 20-mL brown glass vials after adding biochars. KTP and TCS were added simultaneously in bisolute sorption experiments. For isothermal experiments, ratios of initial concentrations ( $C_i$ ) to aqueous solubility ( $S_w$ ) ranged from 0.03 to 0.93 for KTP, and 0.08 to 0.95 for TCS. Solid-to-water ratios (g/mL) were 1:1000 for KTP sorption by WS300, 3:20,000 for KTP sorption by WS700, 1:2000 for TCS sorption by WS300, and 1:10,000 for TCS sorption by WS700. Bisolute sorption with KTP as the primary solute and TCS (7.43  $\text{mg L}^{-1}$ ) as the secondary sorbate (cosolute), and TCS as the primary solute and KTP (39.96  $\text{mg L}^{-1}$ ) as the secondary sorbate was conducted. Bisolute sorption of KTP (41.53  $\text{mg L}^{-1}$ ) with the presence of TCS of 2.60, 5.13, and 7.69  $\text{mg L}^{-1}$  and bisolute sorption of TCS (6.82  $\text{mg L}^{-1}$ ) with the presence of KTP of 15.34, 30.97, and 46.03  $\text{mg L}^{-1}$  were determined to illustrate the effect of secondary sorbate concentrations. The detailed experimental conditions were listed in Table S1 in the Supporting Information.

For all sorption experiments, the pHs of the suspensions were adjusted to 2.0, 7.0, and 10.0 using HCl or NaOH. The pHs were also monitored at the end of the experiments and no significant pH change (within 0.5) was observed between single solute and bisolute systems. Although the two pHs (2.0 and 10.0) are not of significant environmental relevance, sorption study at these pHs can give important insight on species

distribution of KTP and TCS and bisolute sorption mechanisms.

The sample vials were placed on a reciprocal shaker in the dark at 175 rpm and  $25 \pm 1$  °C for 3 days for KTP sorption by WS700 and TCS sorption by WS300 and WS700, and 7 days for KTP sorption by WS300 to reach the apparent equilibrium. After centrifugation (3000 rpm for 15 min for WS300 and WS700, and 12,000 rpm for 10 min for WS300 in succession), the supernatants were taken for further analysis. The final methanol volume in fractions from stock solution was kept at <0.2% (v/v) to avoid co-solvent effects. Duplicates were measured for all the samples. Blank samples without biochar were regularly run to account for the minor solute loss during the experiments.

KTP and TCS were analyzed by a high-performance liquid chromatography (HPLC) with a  $4.6 \times 150$ -mm reverse phase XDB-C18 column and an UV detector (HPLC, Shimadzu Corp, LC-20AT, Japan). KTP was measured using methanol-water (pH was adjusted to 3.0 using acetic acid) (70:30, v/v) as the mobile phase, and TCS was measured using acetonitrile-water (pH was adjusted to 3.0 using acetic acid) (80:20, v/v) as the mobile phase. The flow rate was 1.0  $\text{mL min}^{-1}$ . The determination wavelengths were 257 nm and 280 nm for KTP and TCS, respectively.

### 2.4 Data Analysis

Sorption coefficient ( $K_d$ ,  $\text{L kg}^{-1}$ ) was calculated as:

$$K_d = C_s / C_e \quad (4)$$

where  $C_s$  ( $\text{mg g}^{-1}$ ) is the sorbent loading and  $C_e$  ( $\text{mg L}^{-1}$ ) is the equilibrium aqueous concentration of the sorbate.

Sorption isotherms were fitted with the Freundlich model:

$$C_s = K_F C_e^n \quad (5)$$

where  $K_F$  ( $\text{mg}^{(1-n)} \text{L}^n \text{g}^{-1}$ ) is the Freundlich affinity coefficient and  $n$  is the Freundlich parameter reflecting the nonlinearity of sorption (nonlinearity increases as  $n$  deviates from 1.0).

### 3 Results and Discussion

#### 3.1 Properties of Biochars

From WS300 to WS700, the C content increased; however, the H and O contents decreased (Table 1), indicating an increase in the carbonization degree of biochars (Chen et al. 2012b; Xiao et al. 2014; Sun et al. 2016). The lower atomic ratios of H/C, O/C, and (O + N)/C from WS300 to WS700 suggested the reduction of polar groups and that the biochar was more aromatic. The disappearance of FTIR signals for  $-\text{CH}_2-$ ,  $-\text{C}=\text{O}$ , and other aliphatic functional groups from WS300 to WS700 are in line with the elemental composition results (Fig. 2). The SSA of biochars increased sharply from 6.47 to 605.38  $\text{m}^2 \text{g}^{-1}$  when the pyrolysis temperature increased from 300 to 700  $^{\circ}\text{C}$  (Table 1), which is likely because of the destruction of aliphatic alkyl and ester  $\text{C}=\text{O}$  groups shielding the aromatic structure (Chen and Chen 2009; Keiluweit et al. 2010). Compared with WS300, WS700 has more micropores (IUPAC definition,  $<2 \text{ nm}$ ) (Table 1 and Fig. 3), which provides enhanced internal surface area for sorption.

The surfaces of biochars were mostly negatively charged in the tested pH range (Fig. 4). The point of zero charge ( $\text{pH}_{\text{PZC}}$ ) was estimated to be about 2.0 for both WS300 and WS700 (Table 1 and Fig. 4). Obviously, the zeta potential decreased quickly with increasing solution pH, then began to increase slowly and subsequently decreased with a horizontal S-shape (Fig. 4). Two significant inflection points can be observed (named  $\text{pH}_{\text{d1}}$  and  $\text{pH}_{\text{d2}}$ , marked in Fig. 4), and they were suggested to represent two different types of pH-dependent functional groups on biochars (Fang et al. 2014). Coupled with FTIR spectra of  $-\text{COOH}$  and  $-\text{OH}$  bands on biochars, the  $\text{pH}_{\text{d1}}$  and  $\text{pH}_{\text{d2}}$  correspond to the dissociation of carboxyl and hydroxyl groups,

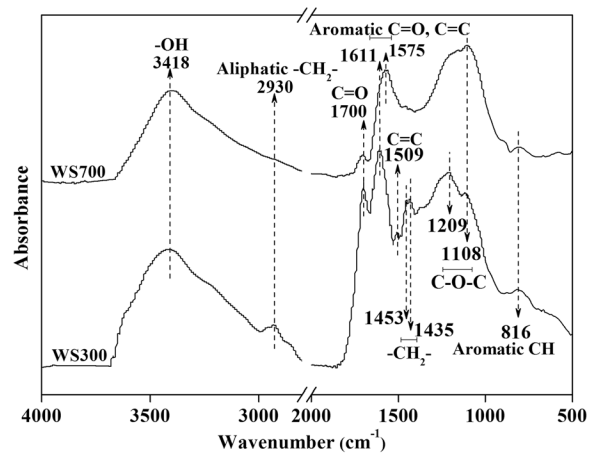


**Fig. 2** FTIR spectra of WS300 and WS700

respectively (Fang et al. 2014). When the pH decreased from 12 to 10, some peaks of zeta potential were found. Similar phenomenon was also observed on other biochars (Fang et al. 2014), but the reason was not clear. Since the inflection points probably represent pH-dependent functional groups on biochars, the peaks may be related to the dissociation of pH-dependent functional groups ( $-\text{COOH}$  or  $-\text{OH}$ ) on biochars (Chen et al. 2014), or addition of a large amount of  $\text{Na}^+$  when  $\text{NaOH}$  was used to adjust solution pH.

#### 3.2 Single Solute Sorption

Sorption isotherms of KTP and TCS by biochars at various pHs in the single solute system are fitted well by the Freundlich model and are nonlinear with  $n$  values varying from 0.12 to 0.60 (Fig. 5 and Table 2). WS700 clearly had higher sorption of KTP and TCS than WS300 under the same conditions (Fig. 5 and Table 2). This could be due to the higher specific surface area of WS700 and suggests that some specific

**Table 1** Properties of WS300 and WS700

Biochar	C (%)	H (%)	N (%)	O <sup>a</sup> (%)	H/C <sup>b</sup>	O/C <sup>c</sup>	(O + N)/C <sup>d</sup>	SSA ( $\text{m}^2 \text{g}^{-1}$ )	Micropore volume ( $\text{cm}^3 \text{g}^{-1}$ )	$\text{pH}_{\text{PZC}}$
WS300	64.88	4.10	0.70	30.33	0.758	0.351	0.360	6.47	0.001	~2.0
WS700	67.82	2.13	0.77	29.28	0.377	0.324	0.333	605.38	0.168	~2.0

Elemental compositions and atomic ratios are on an ash-free basis

<sup>a</sup> Determined by mass balance

<sup>b</sup> Atomic ratio of hydrogen to carbon

<sup>c</sup> Atomic ratio of oxygen to carbon

<sup>d</sup> Atomic ratio of the sum of oxygen and nitrogen to carbon



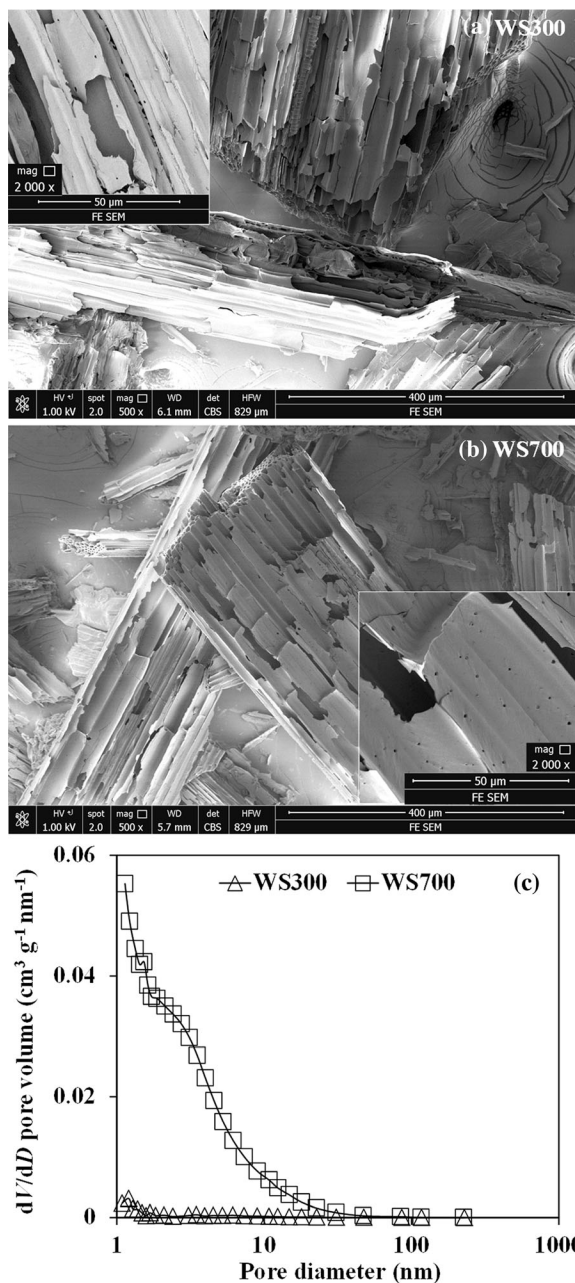


**Fig. 3** SEM images and pore size distribution of WS300 and WS700

interactions may significantly contribute to the sorption (Keiluweit and Kleber 2009).

Moreover, sorption of KTP and TCS tended to decrease with increasing pH from 2.0 to 10.0 (Table 2). The lower sorption obtained upon dissociation could be elucidated by the higher hydrophilicity of anionic species of sorbates, electrostatic repulsion between the

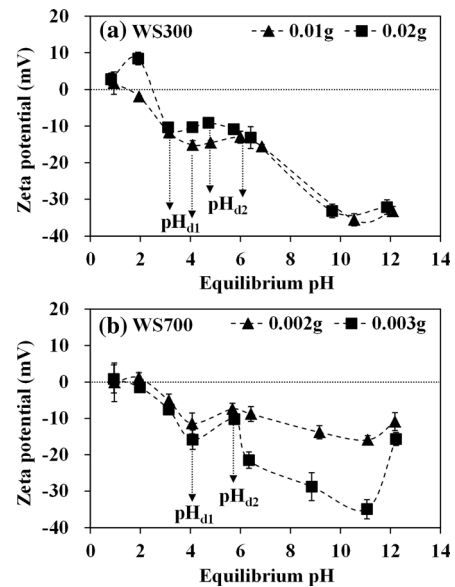


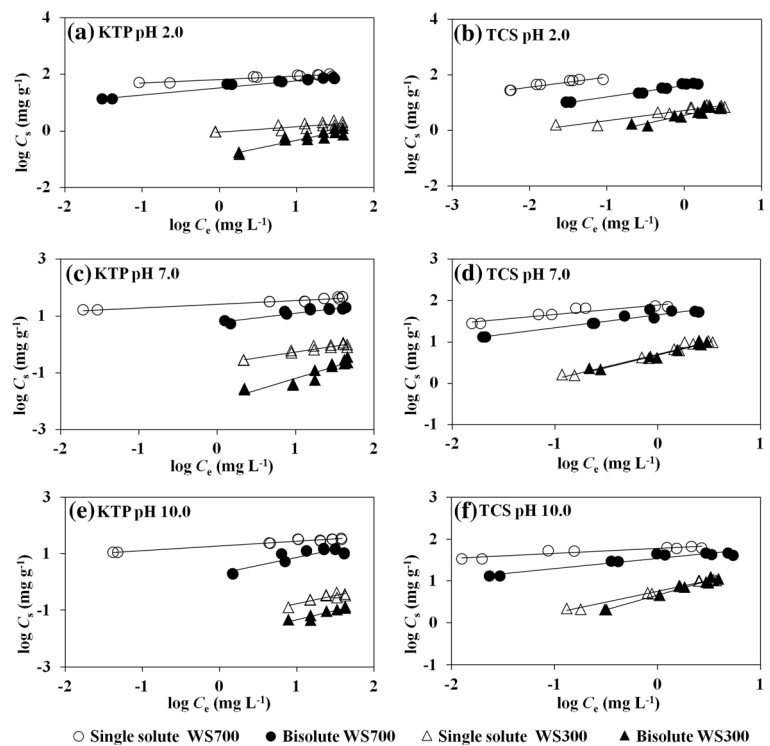
**Fig. 4** Zeta potential of WS300 and WS700 under varying pH

anionic species, and the negatively charged surface of biochars and decreased H-bonding strength between sorbates and biochars due to the dissociation of the O-containing groups of KTP and TCS. However, sorption of KTP and TCS by WS300 with higher O and H contents was markedly less than that by WS700 (Table 1 and Table 2), so H-bonding was not a main mechanism in KTP and TCS sorption. Negative correlation between sorption and the sorbent O and H contents could be because the accessibility of sorption sites reduced due to the formation of water clusters around the O-containing groups at the surface of the sorbent (Franz et al. 2000).

The fraction of  $\text{KTP}^-$  and  $\text{TCS}^-$  was less than 0.4% in the pH range (0.83–2.00) when WS300 and WS700 were positively charged to some extent (Fig. 1), so electrostatic attraction between anionic species and positively charged biochars can be ignored. In addition, the N content in WS300 and WS700 was very small compared to the O content (Table 1); thus, electrostatic attraction between positively charged N groups and anionic species was probably very weak under the experimental conditions.

Sorption nonlinearity was higher in WS700 than in WS300 (see  $n$  values in Table 2). This is because, compared with the highly carbonized WS700, WS300 with a lower degree of carbonization still contains a noncarbonized phase (Chen et al. 2012a). So partition of  $\text{KTP}^0$  and  $\text{TCS}^0$  can occur in the noncarbonized

**Fig. 5** Sorption isotherms of KTP and TCS in single solute (KTP only or TCS only) and bisolute (KTP + TCS) systems. The *black lines* are the Freundlich model fitting results. Initial secondary sorbate concentration ( $\text{mg L}^{-1}$ ) in bisolute systems: KTP, 39.96; TCS, 7.43



phase of WS300 (Fig. 6a). Though partition of hydrophilic  $\text{KTP}^-$  and  $\text{TCS}^-$  is negligible, sorption of anionic species at pH 7.0 or pH 10.0 was still observed.

Recently, a strong charge-assisted H-bond between dissociated aromatic acids and the surface of oxidized carbonized sorbents was suggested (Ni et al. 2011). Sorption is accompanied by proton exchange with water, and an increase in solution pH upon sorption is an indicator for the occurrence of this mechanism. In this study, the increased pH was observed only for KTP sorption by WS700; there was either no change or a slight decrease in the pH for all the other sorption. It is possible that charge-assisted H-bonding occurred for O-containing sorbents, but if it did then it was still not a main mechanism and its contribution to the overall sorption remained small because sorption of KTP and TCS was negatively related to the O content of biochars (Table 1 and Table 2). This could be due to the insufficient O content of biochars for charge-assisted H-bonding to take place (Sigmund et al. 2016).

As the charge-assisted H-bond was ruled out as the main sorption mechanism of anionic species, other specific interactions, such as  $\pi$ - $\pi$  interactions (Zhu and Pignatello 2005; Keiluweit and Kleber 2009), are likely responsible for the uptake of anionic species as well as

neutral species by biochars since both KTP and TCS contain aromatic ring system (Fig. 1). This is supported by the experimental results that WS700 had higher sorption affinity for KTP and TCS than WS300 (Fig. 5 and Table 2). The reason is that WS700 has a higher specific surface area and more aromatic graphite-like structures.

### 3.3 Bisolute Sorption

Different levels of sorption competition between KTP and TCS in the bisolute system were observed at various pHs when sorbates dissociated at different degrees (Fig. 5 and Table 2). This indicated that KTP and TCS have shared sites on biochars for competitive sorption. When the secondary sorbate was added in the bisolute system, the initially high and nonlinear KTP and TCS sorption to WS300 and WS700 declined to yield a lower and less nonlinear sorption at all experimental pHs (Table 2) because of the sorbate displacement (Chiou et al. 2015). Note that the competition strength in KTP sorption when TCS was the secondary sorbate appeared to be minimal at pH 2.0 for WS300 and WS700, and to be maximal at pH 7.0 for WS300 and at pH 10.0 for WS700 (Table 2). Correspondingly, the maximal

**Table 2** Fitted results of the Freundlich model for KTP and TCS sorption in single solute and bisolute systems

Primary sorbate	Biochar	Batch <sup>a</sup>	pH	Freundlich model			log $K_d$ (L kg <sup>-1</sup> ) <sup>b</sup>		Competition strength of secondary sorbate <sup>c</sup>			
				$K_F$ (mg <sup>(1-n)</sup> L <sup>n</sup> g <sup>-1</sup> )	$n$	$R^2$	$C_e = A1$ mg L <sup>-1</sup>	$C_e = A2$ mg L <sup>-1</sup>	B1 (%)	B2 (%)		
KTP	WS300	SS	2.0	0.91	0.19	0.67	2.15	1.83				
		BS	2.0	0.13	0.57	0.86	1.68	1.51	66.51	52.62		
		SS	7.0	0.21	0.41	0.92	1.74	1.50				
		BS	7.0	0.01	0.83	0.87	0.81	0.74	88.15	82.59		
		SS	10.0	0.05	0.57	0.79	1.23	1.06				
		BS	10.0	0.01	0.66	0.88	0.66	0.53	73.05	70.71		
	WS700	SS	2.0	64.21	0.12	0.91	3.93	3.58				
		BS	2.0	32.99	0.25	0.97	3.77	3.47	30.48	21.59		
		SS	7.0	26.34	0.13	0.95	3.55	3.21				
		BS	7.0	6.00	0.33	0.90	3.10	2.83	64.53	57.70		
		SS	10.0	18.89	0.17	0.96	3.44	3.11				
		BS	10.0	2.01	0.57	0.79	2.87	2.70	73.01	60.93		
		TCS	WS300	SS	2.0	5.26	0.37	0.93	3.91	3.72		
				BS	2.0	3.55	0.60	0.88	3.67	3.55	42.52	32.53
SS	7.0			5.10	0.60	0.97	3.83	3.71				
BS	7.0			4.87	0.61	0.97	3.81	3.69	5.08	4.43		
SS	10.0			5.65	0.52	0.99	3.90	3.75				
BS	10.0			4.56	0.70	0.98	3.75	3.66	28.57	19.20		
WS700	SS		2.0	190.72	0.36	0.92	6.17	5.98				
	BS		2.0	40.78	0.41	0.98	5.43	5.25	81.86	81.21		
	SS		7.0	78.70	0.23	0.87	5.13	4.90				
	BS		7.0	45.68	0.32	0.93	4.87	4.66	45.31	41.96		
		SS	10.0	59.65	0.12	0.88	5.04	4.78				
		BS	10.0	34.46	0.24	0.91	4.77	4.54	46.88	42.23		

<sup>a</sup>SS and BS indicate the single solute system and bisolute system experiments, respectively

<sup>b</sup> $K_d$  is the calculated single point sorption coefficient of primary sorbate at  $C_e = A1$  or  $A2$  mg L<sup>-1</sup> using the Freundlich model fitting results. For KTP sorption, A1 is 10.00 and A2 is 25.00. For TCS sorption, A1 is 0.50 and A2 is 1.00 except for the sorption of TCS to WS700 at pH 2.0. For the sorption of TCS to WS700 at pH 2.0, A1 is 0.04 and A2 is 0.08. A1 and A2 used in calculation were in the concentration range of this study

<sup>c</sup>When KTP is the primary sorbate, TCS is the secondary sorbate, and vice versa. Competition strength of secondary sorbate was calculated by  $(K_{d, SS} - K_{d, BS})/K_{d, SS} \times 100\%$  (Zhang et al. 2012).  $K_{d, SS}$  is the  $K_d$  of primary sorbate in the single solute system;  $K_{d, BS}$  is the  $K_d$  of primary sorbate in the bisolute system. B1 was for  $C_e = A1$  mg L<sup>-1</sup> and B2 was for  $C_e = A2$  mg L<sup>-1</sup>

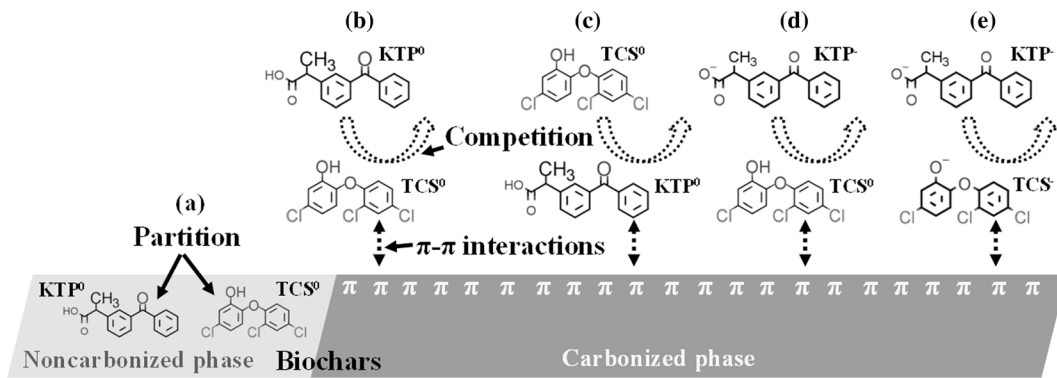
competition strength in TCS sorption when KTP was the secondary sorbate was seen at pH 2.0 for WS300 and WS700, and the minimal competition strength was seen at pH 7.0 for WS300 and WS700 (Table 2).

At pH 2.0, both KTP and TCS existed almost in neutral forms, and were very hydrophobic with log  $D_{OW}$  of 3.17 and 5.42, respectively (Fig. 1). For this reason, the sorption affinity (see log  $K_d$  values in Table 2) of KTP and TCS to biochars at pH 2.0 was high due to strong driving forces. Thus, the sorbate

could resist the sorption competition from competitor or compete for sorption sites at the greatest extent (Fig. 6b, c).

At pH 7.0 and 10.0, most KTP existed as  $KTP^-$ , and the KTP was especially hydrophilic with log  $D_{OW}$  of 0.62 and -1.37, respectively (Fig. 1). This resulted in the lower sorption affinity (Table 2) compared with that at pH 2.0, due to higher hydrophilicity of  $KTP^-$  and electrostatic repulsion between  $KTP^-$  and the negatively charged surface of biochars (Sigmund et al. 2016).





However, TCS in the same conditions at pH 7.0 and 10.0 was very hydrophobic with  $\log D_{OW}$  of 5.39 and 3.55 (Fig. 1b), respectively. As a result, the sorption affinity of TCS to biochars could be higher than that of KTP to biochars (Table 2). Thus, TCS tend to strongly compete with KTP for sorption sites on biochars (Yu and Huang 2005; Sigmund et al. 2016); this led to the highest competition strength at pH 7.0 and 10.0 (Table 2, Fig. 6d, e). The minimum competition strength in TCS sorption caused by KTP at pH 7.0 (Table 2) can be elucidated for the similar reason that it was difficult

for KTP with less hydrophobicity to compete with TCS for sorption sites on biochars.

Since TCS was more competitive than KTP due to its higher hydrophobicity, the sum of KTP and TCS sorption in the bisolute system was calculated and compared with individual KTP sorption in molar equivalents to further probe the mechanisms of competition. The difference between the single solute sorption and sum of bisolute sorption was smaller on WS700 than that on WS300 (Fig. S1 in the Supporting Information). This is probably because partition of neutral TCS can occur in

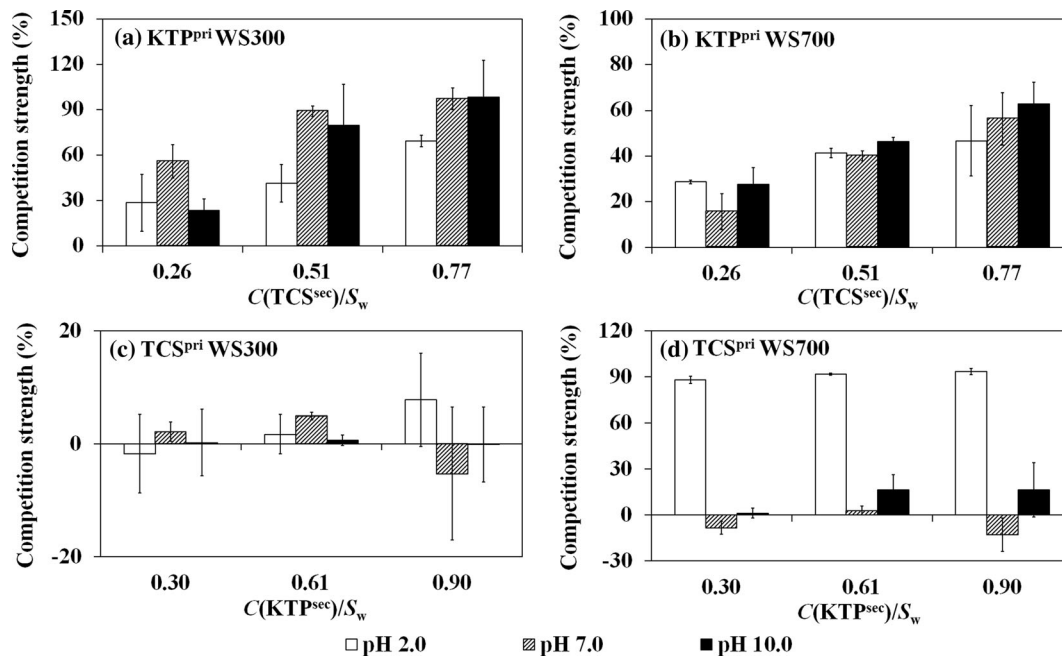


**Fig. 7** Effect of secondary sorbate (TCS<sup>sec</sup> or KTP<sup>sec</sup>) concentration on sorption of primary sorbate (KTP<sup>pri</sup> or TCS<sup>pri</sup>) by WS300 and WS700. Competition strength of secondary sorbate was calculated by  $(K_{d, SS} - K_{d, BS})/K_{d, SS} \times 100\%$  (Zhang et al. 2012).  $K_{d, SS}$

is the  $K_d$  of primary sorbate in the single solute system;  $K_{d, BS}$  is the  $K_d$  of primary sorbate in the bisolute system. Initial primary sorbate concentration (mg L<sup>-1</sup>): KTP, 41.53; TCS, 6.82

the noncarbonized phase of WS300 with lower degree of carbonization.

At high KTP concentrations, the sum of KTP and TCS sorption on WS700 was not significantly different from individual KTP sorption on it (Fig. S1 in the Supporting Information), which showed that 1 M TCS molecules may replace approximately 1 M KTP molecules. This was similar with the competitive sorption among benzene, toluene, and nitrobenzene on charcoal, in which these molecules could replace each other in a molar ratio of 1:1:1, indicating 100% overlapping of sorption sites (Sander and Pignatello 2005).

Effect of secondary sorbate concentration on sorption of primary sorbate was also evaluated. Results showed that the competition between KTP and TCS increased with increasing concentration of TCS (secondary sorbate) at all pHs when KTP was the primary sorbate (Fig. 7a, b). However, there was no competition or very weak competition between KTP and TCS with increasing concentration of KTP (secondary sorbate) when TCS was the primary sorbate except for the TCS sorption by WS700 at pH 2.0 (Fig. 7c, d). It is elucidated that TCS (with higher hydrophobicity) can compete with KTP (with lower hydrophobicity) for sorption sites easily, so competition increased with increasing TCS concentration as more KTP on sorption sites was replaced by TCS (Fig. 7a, b). Similarly, TCS occupying sorption sites can be hardly replaced by KTP as the hydrophobicity of KTP was lower than that of TCS. Consequently, insignificant competition between KTP and TCS was observed at pH 7.0 and pH 10.0 (Fig. 7c, d).

For neutral aromatic sorbates, it is well accepted that partition exists in noncarbonized biochar or biochar with low degree of carbonization and specific adsorption interactions (such as  $\pi$ - $\pi$  interactions) dominate sorption of carbonized biochar (Chen et al. 2012a; Keiluweit and Kleber 2009; Sigmund et al. 2016). Competitive sorption cannot happen through partition but can happen through adsorption interactions which are related to the available sites on sorbent (Yu and Huang 2005; Chiou et al. 2015). Therefore, sorption competition between KTP and TCS was more obvious on WS700 than that on WS300 at pH 2.0 when TCS was the primary sorbate (Fig. 7c, d), probably because neutral KTP was mainly sorbed through partition (noncompetitive) in noncarbonized phase of WS300 with lower degree of carbonization (Fig. 6a), but through specific adsorption interactions (competitive) on carbonized phase of WS700 with higher degree of carbonization (Fig. 6c).

## 4 Conclusions

WS700 with higher degree of carbonization had higher sorption coefficient ( $K_d$ ) and nonlinearity than WS300 in the single solute system. In the bisolute system, no competitive effect was observed for partition of neutral KTP and TCS in the noncarbonized phase of WS300, but they competed for the sorption sites on the carbonized phase of WS300 and WS700, where  $\pi$ - $\pi$  interaction was proposed to be the main mechanism. The competition in the bisolute system varied with degree of dissociation of KTP and TCS, and led to a lower nonlinear sorption compared with that in the single solute system. TCS was more competitive than KTP due to its higher hydrophobicity, and sorption inhibition of KTP was enhanced with increasing TCS concentration. The effects of environmental factors, such as bivalent and multivalent cations and dissolved organic matter on bisolute sorption should be studied in order to further understand the mechanisms.

**Acknowledgements** This research was supported by the National Natural Science Foundation of China (No. 41472231 and No. 51238001) and Beijing Natural Science Foundation (No. 8162021).

## References

- Behera, S. K., Oh, S.-Y., & Park, H.-S. (2010). Sorption of triclosan onto activated carbon, kaolinite and montmorillonite: effects of pH, ionic strength, and humic acid. *Journal of Hazardous Materials*, 179(1–3), 684–691.
- Cederlund, H., Börjesson, E., Lundberg, D., & Stenström, J. (2016). Adsorption of pesticides with different chemical properties to a wood biochar treated with heat and iron. *Water, Air, and Soil Pollution*, 227(6), 203.
- Chen, B., & Chen, Z. (2009). Sorption of naphthalene and 1-naphthol by biochars of orange peels with different pyrolytic temperatures. *Chemosphere*, 76(1), 127–133.
- Chen, B., Zhou, D., & Zhu, L. (2008). Transitional adsorption and partition of nonpolar and polar aromatic contaminants by biochars of pine needles with different pyrolytic temperatures. *Environmental Science and Technology*, 42(14), 5137–5143.
- Chen, Z., Chen, B., & Chiou, C. T. (2012a). Fast and slow rates of naphthalene sorption to biochars produced at different temperatures. *Environmental Science and Technology*, 46(20), 11104–11111.
- Chen, Z., Chen, B., Zhou, D., & Chen, W. (2012b). Bisolute sorption and thermodynamic behavior of organic pollutants to biomass-derived biochars at two pyrolytic temperatures. *Environmental Science and Technology*, 46(22), 12476–12483.

- Chen, Z., Xiao, X., Chen, B., & Zhu, L. (2014). Quantification of chemical states, dissociation constants and contents of oxygen-containing groups on the surface of biochars produced at different temperatures. *Environmental Science & Technology*, *49*(1), 309–317.
- Chiou, C. T., Cheng, J., Hung, W. N., Chen, B., & Lin, T. F. (2015). Resolution of adsorption and partition components of organic compounds on black carbons. *Environmental Science and Technology*, *49*(15), 148–157.
- Cho, H.-H., Huang, H., & Schwab, K. (2011). Effects of solution chemistry on the adsorption of ibuprofen and triclosan onto carbon nanotubes. *Langmuir*, *27*(21), 12960–12967.
- Daughton, C. G., & Ternes, T. A. (1999). Pharmaceuticals and personal care products in the environment: agents of subtle change? *Environmental Health Perspectives*, *107*(6), 907–938.
- Dodgen, L. K., Kelly, W. R., Panno, S. V., Taylor, S. J., Armstrong, D. L., Wiles, K. N., et al. (2016). Characterizing pharmaceutical, personal care product, and hormone contamination in a karst aquifer of southwestern Illinois, USA, using water quality and stream flow parameters. *Science of the Total Environment*, *578*, 281–289.
- Fang, Q., Chen, B., Lin, Y., & Guan, Y. (2014). Aromatic and hydrophobic surfaces of wood-derived biochar enhance perchlorate adsorption via hydrogen bonding to oxygen-containing organic groups. *Environmental Science and Technology*, *48*(1), 279–288.
- Franz, M., Arafat, H. A., & Pinto, N. G. (2000). Effect of chemical surface heterogeneity on the adsorption mechanism of dissolved aromatics on activated carbon. *Carbon*, *38*(13), 1807–1819.
- József, D., Margit, V., & Gyula, Z. (2012). Biofilm controlled sorption of selected acidic drugs on river sediments characterized by different organic carbon content. *Chemosphere*, *87*(2), 105–110.
- Jung, C., Boateng, L. K., Flora, J. R. V., Oh, J., Braswell, M. C., Son, A., et al. (2015). Competitive adsorption of selected non-steroidal anti-inflammatory drugs on activated biochars: experimental and molecular modeling study. *Chemical Engineering Journal*, *264*, 1–9.
- Kah, M., & Brown, C. D. (2008). Log D: lipophilicity for ionisable compounds. *Chemosphere*, *72*(10), 1401–1408.
- Keiluweit, M., & Kleber, M. (2009). Molecular-level interactions in soils and sediments: the role of aromatic  $\pi$ -systems. *Environmental Science and Technology*, *43*(10), 3421–3429.
- Keiluweit, M., Nico, P. S., Johnson, M. G., & Kleber, M. (2010). Dynamic molecular structure of plant biomass-derived black carbon (biochar). *Environmental Science and Technology*, *44*(4), 1247–1253.
- Kočárek, M., Kodešová, R., Vondráčková, L., Golovko, O., Fér, M., Klement, A., et al. (2016). Simultaneous sorption of four ionizable pharmaceuticals in different horizons of three soil types. *Environmental Pollution*, *218*, 563–573.
- Kolpin, D. W., Furlong, E. T., Meyer, M. T., Thurman, E. M., Zaugg, S. D., Barber, L. B., et al. (2002). Pharmaceuticals, hormones, and other organic wastewater contaminants in U.S. streams, 1999–2000: a national reconnaissance. *Environmental Science and Technology*, *36*(6), 1202–1211.
- Kumari, K. G. I. D., Moldrup, P., Paradelo, M., & Jonge, L. W. D. (2014). Phenanthrene sorption on biochar-amended soils: application rate, aging, and physicochemical properties of soil. *Water, Air, and Soil Pollution*, *225*(9), 2105.
- Ni, J., Pignatello, J. J., & Xing, B. (2011). Adsorption of aromatic carboxylate ions to black carbon (biochar) is accompanied by proton exchange with water. *Environmental Science and Technology*, *45*(21), 9240–9248.
- Pan, B., & Xing, B. (2010). Competitive and complementary adsorption of bisphenol A and 17  $\alpha$ -ethinyl estradiol on carbon nanomaterials. *Journal of Agricultural and Food Chemistry*, *58*(14), 8338–8343.
- Reiss, R., Mackay, N., Habig, C., & Griffin, J. (2002). An ecological risk assessment for triclosan in lotic systems following discharge from wastewater treatment plants in the United States. *Environmental Toxicology & Chemistry*, *21*(11), 2483–2492.
- Sander, M., & Pignatello, J. J. (2005). Characterization of charcoal adsorption sites for aromatic compounds: insights drawn from single-solute and bi-solute competitive experiments. *Environmental Science & Technology*, *39*(6), 1606–1615.
- Sigmund, G., Sun, H., Hofmann, T., & Kah, M. (2016). Predicting the sorption of aromatic acids to non-carbonized and carbonized sorbents. *Environmental Science and Technology*, *50*(7), 3641–3648.
- Sun, K., Kang, M., Ro, K. S., Libra, J. A., Zhao, Y., & Xing, B. (2016). Variation in sorption of propiconazole with biochars: the effect of temperature, mineral, molecular structure, and nano-porosity. *Chemosphere*, *142*, 56–63.
- Tan, X., Liu, Y., Zeng, G., Xin, W., Hu, X., Gu, Y., et al. (2015). Application of biochar for the removal of pollutants from aqueous solutions. *Chemosphere*, *125*, 70–85.
- Tijani, J. O., Fatoba, O. O., & Petrik, L. F. (2013). A review of pharmaceuticals and endocrine-disrupting compounds: sources, effects, removal, and detections. *Water, Air, and Soil Pollution*, *224*(11), 1–29.
- Tixier, C., Singer, H. P., Oellers, S., & Muller, S. R. (2003). Occurrence and fate of carbamazepine, clofibric acid, diclofenac, ibuprofen, ketoprofen, and naproxen in surface waters. *Environmental Science and Technology*, *37*(6), 1061–1068.
- Wang, P., Yin, Y., Guo, Y., & Wang, C. (2016). Preponderant adsorption for chlorpyrifos over atrazine by wheat straw-derived biochar: experimental and theoretical studies. *RSC Advances*, *6*(13), 10615–10624.
- Xiao, L., Bi, E., Du, B., Zhao, X., & Xing, C. (2014). Surface characterization of maize-straw-derived biochars and their sorption performance for MTBE and benzene. *Environmental Earth Sciences*, *71*(12), 5195–5205.
- Xing, B., Pignatello, J. J., & Gigliotti, B. (1996). Competitive sorption between atrazine and other organic compounds in soils and model sorbents. *Environmental Science and Technology*, *31*(5), 2432–2440.
- Xu, J., Wu, L., Chen, W., & Chang, A. C. (2009). Adsorption and degradation of ketoprofen in soils. *Journal of Environmental Quality*, *38*(38), 1177–1182.
- Yu, Z., & Huang, W. (2005). Competitive sorption between 17 $\alpha$ -ethinyl estradiol and naphthalene/phenanthrene by sediments. *Environmental Science and Technology*, *39*(13), 4878–4885.
- Zhang, D., Pan, B., Wu, M., Zhang, H., Peng, H., Ning, P., et al. (2012). Cosorption of organic chemicals with different properties: their shared and different sorption sites. *Environmental Pollution*, *160*(1), 178–184.
- Zhu, D., & Pignatello, J. J. (2005). Characterization of aromatic compound sorptive interactions with black carbon (charcoal) assisted by graphite as a model. *Environmental Science and Technology*, *39*(7), 2033–2041.